Complex Dynamics during Metal Dissolution: From Intrinsic to Faceted Anomalous Scaling

P. Córdoba-Torres,* T. J. Mesquita,† I. N. Bastos,‡ and R. P. Nogueira

UMR5266 and 5631 INP Grenoble-CNRS-UJF, SIMAP and LEPMI, BP 75, 38402 St Martin d'Hères, France

(Received 26 September 2008; published 6 February 2009)

The kinetic roughening of dissolving polycrystalline pure iron has been studied. A depth analysis of surface images has shown two consecutive growth regimes characterized by different scaling anomalous properties: an initial intrinsic anomalous scaling evolving in the thick film limit towards the theoretically conjectured faceted anomalous scaling. This represents the first experimental evidence of such scaling as well as of such transition. The dynamics presented here may account for the striped surface pattern observed during the evolution of metals or alloys in a large number of processes.

DOI: 10.1103/PhysRevLett.102.055504 PACS numbers: 81.10.Aj, 05.40.−a, 68.55.−a, 82.45.Qr

In the past decade, a great deal of theoretical [1–6] and experimental [7–16] effort has been devoted to the study of anomalous scaling in kinetic surface roughening. To characterize it, generic dynamic scaling forms for the correlation functions of the system have been proposed [4]. The basic function to consider in real space is the local width $w(l, t)$, defined by the rms surface height fluctuations in square windows of size l on a system of lateral size L. The generic dynamic scaling proposed for it can be written as $w(l, t) \sim l^{\alpha} f(l/t^{1/z})$, with α and z being, respectively, the roughness and the dynamic exponent of the growth, and where the scaling function $f(u)$ has the general form $f(u) \sim u^{-(\alpha-\alpha_{\mathrm{loc}})}$ for $u \ll 1$ and $f(u) \sim u^{-\alpha}$ for $u \gg 1$. An independent local roughness exponent α_{loc} characterizes scaling at local scales. The complete characterization of the scaling properties of a growing surface must also consider the scaling of the power spectrum or structure factor $S(k, t)$, proposed as $S(k, t) \sim k^{-(2\alpha+d)} s(kt^{1/z})$, with the scaling function $s(u) \sim u^{2(\alpha-\alpha_s)}$ for $u \gg 1$ and $s(u) \sim u^{2\alpha+d}$ for $u \ll 1$, where d is the topological dimension of the surface and α_s is known as the spectral roughness exponent. It has been theoretically argued [4] that this generic scaling ansatz includes all the existing scaling behaviors in scale invariant roughening, normal or anomalous, which can be derived as subclasses of it and grouped in the following classification:

$$\begin{aligned} \alpha_s < 1 \Rightarrow \alpha_{\mathrm{loc}} = \alpha_s \begin{cases} \alpha_s = \alpha \Rightarrow \text{Family-Vicsek} \\ \alpha_s \neq \alpha \Rightarrow \text{intrinsic} \end{cases} \\ \alpha_s > 1 \Rightarrow \alpha_{\mathrm{loc}} = 1 \begin{cases} \alpha_s = \alpha \Rightarrow \text{super-rough} \\ \alpha_s \neq \alpha \Rightarrow \text{faceted.} \end{cases} \end{aligned} \tag{1}$$

The physical origin of the different forms of anomalous scaling has not yet been clearly resolved, and it is still a matter of great interest. Super-roughening and intrinsic anomalous roughening have been found [1,3,6] to be related with a nontrivial dynamics of the local slope fluctuations: $\overline{\langle (\nabla h)^2 \rangle} \sim t^{2\kappa}$, where $\kappa > 0$ and $\alpha - \alpha_{\mathrm{loc}} = z\kappa$. In particular, for the intrinsic case, it has been theoretically argued [1] and observed in discrete models [5] and experiments [8,10–12] that it is due to nonlocal effects on the growth. The third type of anomalous scaling has been predicted theoretically [4] and observed in some growth models [4,17], but as far as we know, it has not yet been experimentally reported. It has proved to account for the coarsening kinetics of faceted interfaces resulting from models for self-organized depinning and interface growth in disordered media [17,18]. Another important question addressed here and less explored in previous experimental works concerns the evolution of anomalous scaling in time [5,12,15], especially in the thick film limit. In this Letter, we show that an anomalous scaling behavior can evolve in the thick film limit towards a different anomalous class, and we report the first experimental evidence of the theoretically conjectured faceted anomalous scaling.

We have studied electrodissolution of pure polycrystalline iron (99.99%) at constant current density. For details of the experimental setup, the reader is referred to Ref. [16]. To explore the thick film regime, the electrode was submitted to galvanostatic high anodic dissolution ($J = 12.7\ \mathrm{mA\,cm^{-2}}$) up to different dissolution charges yielding the following depths of attack: 0.94, 1.68, 2.81, 4.68, 8.42, 14.03, and 25.25 μm. Surface topography was measured using a Veeco D3100 AFM in tapping mode. Images of two different scan lateral sizes l^*: 30 and 5 μm, were acquired, both with the same 512×512 pixel resolution. To gain statistics in the scaling analysis and check reproducibility, several regions of the sample were imaged with these two scan sizes, thus addressing different grains. Local width $w(l, t)$ was obtained from the average over all square windows of side $l \leq l^*$ covering a particular image, and then averaged again over all the images obtained with the same scan size at the same dissolution charge. The minimum l considered in our analysis is that corresponding to 4 times the dimension of a single image pixel, i.e., $l \geq 4l^*/512$. For each dissolution charge, different images of 30 μm (5–10) and 5 μm (10–15) were recorded up to obtain a good coincidence, in terms of overlapping values of l, between the two curves $w(l, t)$ vs l. Power spectrum

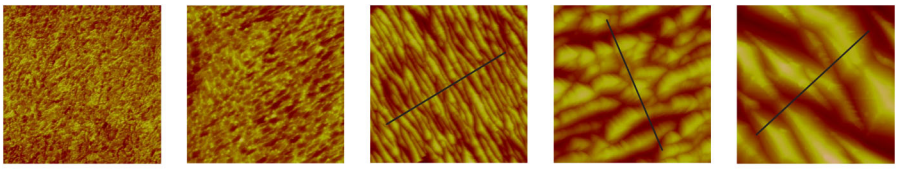

FIG. 1 (color online). Sequence of 30 μm $\times$ 30 μm (a)–(c) and 20 μm $\times$ 20 μm (d), (e) top view AFM images after different increasing dissolution charges. Solid lines in images (c) to (e) indicate the direction of the cross sections taken for the $d = 1$ scaling analysis.

$S(k, t)$ was calculated from the height data of the largest window ($l^* = 30$ μm) and then averaged over different windows.

In Fig. 1, we display a representative time sequence of AFM images corresponding to the largest window investigated in each charge. Surface topography evolution can be divided into two consecutive growth regimes. Regime I comprises initial dissolution charges up to 4.5 C [Figs. 1(a) to 1(c)]. The analysis of the data has shown that local width and power spectrum increases with dissolution time at local scales ($l \ll t^{1/z}$), as expected in the intrinsic anomalous scaling: $w \sim l^{\alpha_{\rm loc}} t^{\kappa}$ and $S(k, t) \sim k^{-(2\alpha_s+2)} t^{2(\alpha-\alpha_s)/z}$. The scaling exponents have been estimated in different ways. The collapses of local width and power spectrum have been displayed in Fig. 2. In spite of the fact that both local roughness and spectral exponents seems to increase slightly with the dissolution time (not shown here), very good collapses are obtained by using exponents $\alpha = 1.6$ and $z = 2.0$ for the local width, and $\alpha = 1.6$ and $z = 2.3$ for the structure factor. When measured for the largest dissolution time ($Q = 4.5$ C), anomalous exponents take the value $\alpha_{\rm loc} = \alpha_s = 0.9$. According to those results, a growth exponent $\beta = \alpha/z \approx 0.7$–$0.8$ is expected. Figure 3 shows the scaling of the saturated local width [$w_{\rm sat}(t) = w(l, t)$ for $l \gg t^{1/z}$] with the dissolution charge. It behaves according to the predicted power law $\sim t^{\beta}$ with $\beta = 0.78$, in excellent agreement with the previous estimate. To add more consistency to the results, we have measured the exponent κ characterizing the anomalous scaling of the average local slope (inset of Fig. 3). It gives $\kappa = 0.34$ in good agreement with the prediction from the collapses: $\kappa = (\alpha - \alpha_{\rm loc})/z = 0.30$–$0.35$. We then conclude that in regime I, metal surface displays an intrinsic anomalous roughening.

Regime II corresponds to charges from 4.5 C [Figs. 1(c) to 1(e)]. Because of the high morphological anisotropy, the dynamic scaling in the orthogonal direction to the anisotropy (case $d = 1$)—indicated by horizontal lines in Fig. 1—has also been analyzed. For that purpose, 20 different cross sections with the same length $l^* = 20$ μm were considered in each AFM image, thus giving an ensemble of 100 profiles approximately for each dissolution charge. For the scaling analysis of the local width, we have divided each profile in linear segments of size $l \leq l^*$. An unusual anomalous behavior has been observed in both dimensions. Local roughness unexpectedly decreases with the dissolu-

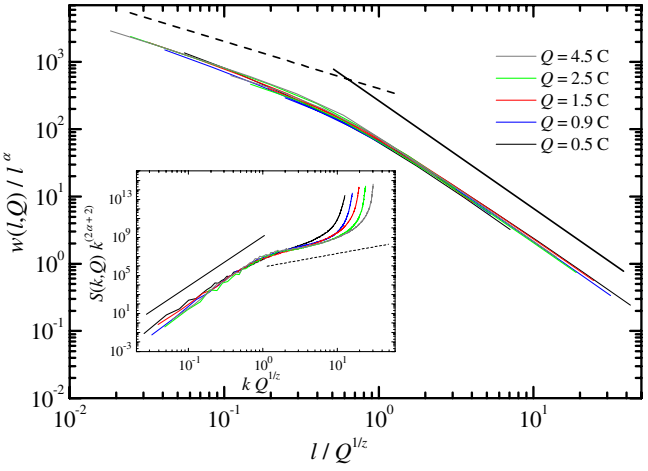

FIG. 2 (color online). Best collapse of local width for dissolution charges of regime I. Exponents used are $\alpha = 1.6$ and $z = 2$. The straight lines have slopes -0.7 (dashed line) and -1.6 (solid line). The inset shows the best collapse of the corresponding power spectrum, obtained by using exponents $\alpha = 1.6$ and $z = 2.3$. The straight lines have slopes 1.4 (dashed line) and 5.2 (solid line).

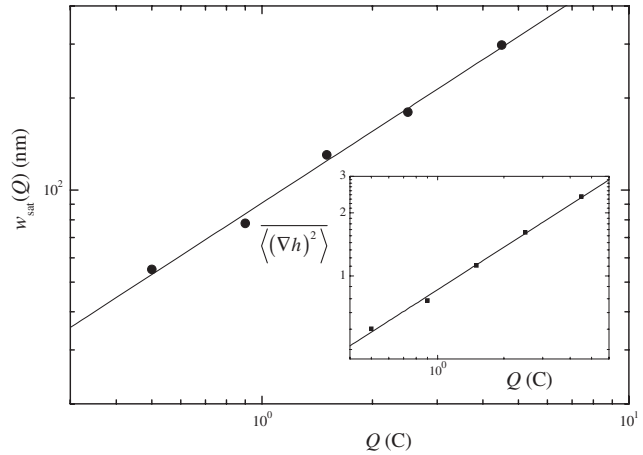

FIG. 3. Saturated local width for different dissolution charges of regime I. Fitting straight line has slope $\beta = 0.78 \pm 0.03$. The inset shows the average local slope obtained from the analysis of the smallest windows ($l^* = 5$ μm) for the same dissolution charges. Fitting straight line has slope 0.68 ± 0.02.

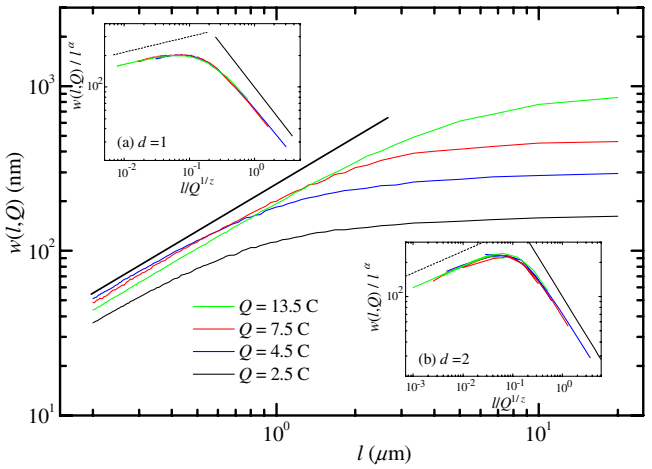

FIG. 4 (color online). Local surface width measured from cross sections ($d = 1$) for different dissolution charges. The solid straight line is plotted to guide the eyes and has slope 0.95. Inset (a) shows the best data collapse for $Q \geq 4.5$ C (Regime II), obtained from exponents $\alpha = z = 0.8$. The straight lines have slopes 0.15 (dashed line) and -0.8 (solid line). Inset (b) shows the best collapse of local width for $d = 2$ and same dissolution charges. Exponents used are $\alpha = z = 0.71$. The straight lines have slopes 0.19 (dashed line) and -0.71 (solid line).

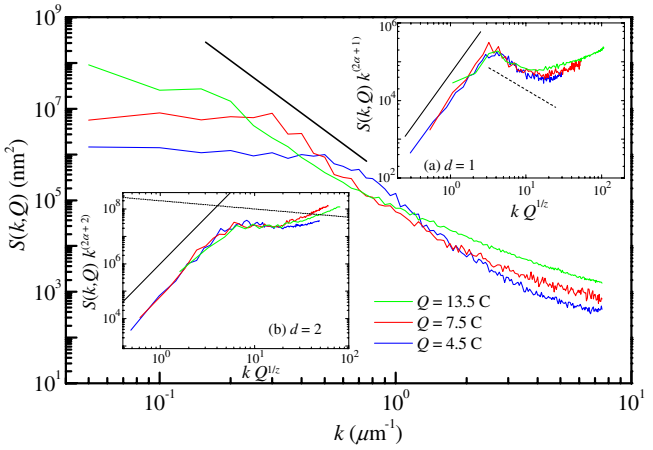

FIG. 5 (color online). Power spectrum of cross sections ($d = 1$) of size 20 μm for different dissolution charges of regime II. The straight segment has slope -3.8 and corresponds to $\alpha_s = 1.4$. Inset (a) shows the best data collapse with exponents $\alpha = z = 0.85$. The straight lines have slopes -1.1 (dashed line) and 2.7 (solid line). Inset (b) shows the best collapse for $d = 2$ with $\alpha = z = 0.75$. The straight lines have slopes -0.3 (dashed line) and 3.5 (solid line).

tion time at small scales ($l \ll t^{1/z}$), as shown in Fig. 4 for the $d = 1$ analysis, whereas the expected increasing is observed for larger scales. To highlight the change in the scaling behavior between regime I and regime II, the result from $Q = 2.5$ C (regime I) has also been plotted for comparison. This anomalous behavior is due to the fact that $\alpha < \alpha_{\mathrm{loc}}$. The collapse for each dimension has been displayed in the insets of Fig. 4. For $d = 1$, it is optimal by using the exponents $\alpha = z = 0.8$, whereas for $d = 2$, we have employed $\alpha = z = 0.71$. Again, the local roughness exponent slightly increases with dissolution time; for the largest charge studied, it takes the value $\alpha_{\mathrm{loc}} = 0.95$ ($d = 1$) and $\alpha_{\mathrm{loc}} = 0.9$ ($d = 2$). For the power spectrum, shown in Fig. 5, a similar effect is observed. As dissolution time increases, the curves seem to shift downward for enough small momenta k just before the saturation is reached. This anomalous power-law displacement in time indicates that $\alpha < \alpha_s$. In $d = 1$, the decay of $S(k, t)$ for long times and small momenta gives an estimate of $\alpha_s = 1.4$ whereas it is $\alpha_s = 0.9$ in $d = 2$. The best data collapses have been shown in the insets of Fig. 5 and have been obtained by using exponents $\alpha = z = 0.85$ ($d = 1$) and $\alpha = z = 0.75$ ($d = 2$). Results from $d = 1$ are in excellent agreement with the anomalous scaling ansatz for faceted surfaces. The $d = 2$ case is not so evident since scaling exponents do not fully match scaling relations for faceted scaling. Estimates of anomalous exponents α_{loc} and α_s are close to the critical value 1 that would indicate the presence of a faceted anomalous scaling. They might be underestimated due to the anisotropic character of the pattern since in the $d = 2$ analysis, all directions are averaged, including those that are not faceted that much. On the other hand, the fact that both α_{loc} and α_s seem to increase with the dissolution charge suggests the possibility that exponent estimates might be affected by the crossover between the two roughening regimes and that for larger dissolution charges, their values might approach to 1, thus indicating a faceted anomalous scaling. We tried to explore larger dissolution charges, but in that case, huge surface instabilities in the form of growing pits appeared, thus modifying surface topography.

Since that scaling has been related with the coarsening dynamics of faceted surfaces, we have also analyzed the

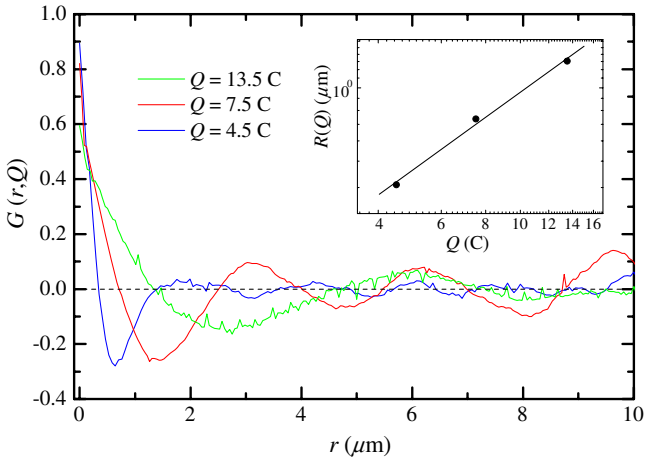

FIG. 6 (color online). Decay of the slope-slope correlation function in cross sections and for dissolution charges of regime II. The inset shows the evolution of the lateral mound size for the three charges considered. Fitting straight line has slope 1.24 ± 0.09.

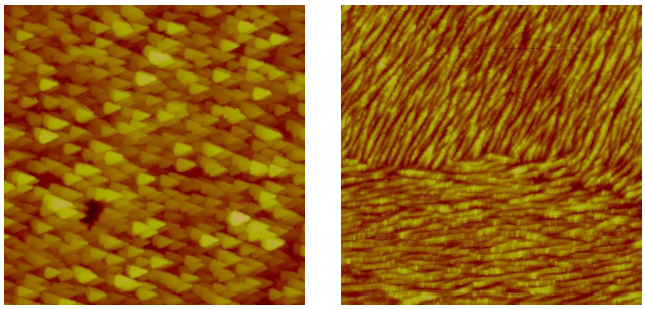

(a) (b)

FIG. 7 (color online). (a) Pyramidal formations in regime I ($l = 30$ μm). (b) Image of the electrode surface displaying two neighboring grains ($l = 10$ μm).

kinetics of the lateral mound size $R(t)$, obtained from the first zero of the slope-slope correlation function $G(r, t) = \langle \overline{\nabla h(\mathbf{x}, t)} \nabla h(\mathbf{x} + r, t) \rangle$. The coarsening length growth is expected to follow a power law $R(t) \sim t^{1/z_{\text{coarse}}}$, with the coarsening exponent z_{coarse} given by the dynamic exponent $z_{\text{coarse}} = z$. In Fig. 6, we show the decay of the slope-slope correlation function calculated from the cross sections of the three charges considered. The growth of the correlation length has been shown in the inset. Data fit gives a coarsening exponent $z_{\text{coarse}} = 0.81$ which agrees with the value of z obtained from the collapses of w and S for $d = 1$. It is worth noticing that the average surface slope, given by $G(0, t)$, behaves anomalously—decreases—with time, in contrast with the power-law growth $\langle \overline{(\nabla h)^2} \rangle \sim t^{2\kappa}$ expected for intrinsic anomalous roughening and super-roughening [1,3,6].

In our opinion, the origin of the initial intrinsic anomalous roughening lies in the strong anisotropic nonlocal growth produced by the differences in the dissolution rates of the different crystallographic directions present in a given texture. Anisotropic dissolution thus acts, exposing close packed crystalline planes—more resistive to dissolution—that pin the surface, whereas it is depinned along crystal directions less packed. This mechanism is probably coupled with surface diffusion and related nonlocal effects such as Schwoebel-barriers [19], and both lead to the initial formation of pyramidal structures with smooth faceted walls, which is consistent with the value $\alpha_{\text{local}} \sim 1$ [see top view AFM image displayed in Fig. 7(a)]. After a certain time, those pyramids commence to line up in a particular direction giving rise to a highly anisotropic pattern [Fig. 1(c)]. Such striped morphology has been observed on metallic surfaces grown by sputter deposition [19] or corrosion [20] and seems to be a result of the underlying crystal structure, with the anisotropy direction being texture dependent, as shown in Fig. 7(b). Finally, the coalescence of the stripes along the direction orthogonal to the anisotropy leads to the development of a faceted surface [regime II, Fig. 1(e)], and its coarsening dynamics results in the conjectured faceted anomalous roughening. It is worth recalling that dynamic scaling presented here is intragranular and does not take into account intergranular effects [19,21]. Furthermore, not all the grains addressed in our study exhibited the pattern. In fact, dissolution resistant grains appeared as high terraces [20] with rare morphologies and were disregarded in the present study.

P. C. T.'s leave is supported by the Program José Castillejo of the Ministerio de Educación y Ciencia (Spain). T. J. M.'s leave is supported by the Program BRAFITEC.

*Corresponding author: pcordoba@dfmf.uned.es. On leave from Departamento de Física Matemática y de Fluidos, UNED, Spain
†On leave from Universidade de Sao Carlos, Brazil.
‡On leave from Instituto Politécnico, UERJ, Brazil.

[1] J. M. López, M. Castro, and R. Gallego, Phys. Rev. Lett. **94**, 166103 (2005).
[2] R. Cuerno and M. Castro, Phys. Rev. Lett. **87**, 236103 (2001).
[3] J. M. López, Phys. Rev. Lett. **83**, 4594 (1999).
[4] J. J. Ramasco, J. M. López, and M. A. Rodríguez, Phys. Rev. Lett. **84**, 2199 (2000).
[5] M. Castro *et al.*, Phys. Rev. E **57**, R2491 (1998).
[6] J. Krug, Phys. Rev. Lett. **72**, 2907 (1994).
[7] S. Yim and T. S. Jones, Phys. Rev. B **73**, 161305(R) (2006).
[8] B. A. Sperling and J. R. Abelson, J. Appl. Phys. **101**, 024915 (2007).
[9] J. H. Jeffries, J.-K. Zuo, and M. M. Craig, Phys. Rev. Lett. **76**, 4931 (1996).
[10] M. A. Auger *et al.*, Phys. Rev. B **73**, 045436 (2006); M. A. Auger *et al.*, J. Appl. Phys. **97**, 123528 (2005).
[11] S. Huo and W. Schwarzacher, Phys. Rev. Lett. **86**, 256 (2001).
[12] M. C. Lafouresse, P. J. Heard, and W. Schwarzacher, Phys. Rev. Lett. **98**, 236101 (2007).
[13] M. Saitou, Phys. Rev. B **66**, 073416 (2002).
[14] A. G. Muñoz, M. E. Vela, and R. C. Salvarezza, Langmuir **21**, 9238 (2005).
[15] J. Soriano *et al.*, Phys. Rev. Lett. **89**, 026102 (2002).
[16] P. Córdoba-Torres, I. N. Bastos, and R. P. Nogueira, Phys. Rev. E **77**, 031602 (2008).
[17] I. G. Szendro, J. M. López, and M. A. Rodríguez, Phys. Rev. E **76**, 011603 (2007).
[18] K. Sneppen, Phys. Rev. Lett. **69**, 3539 (1992).
[19] A. E. Lita and J. E. Sanchez, Jr., Phys. Rev. B **61**, 7692 (2000).
[20] C. A. Schuh, K. Anderson, and C. Orme, Surf. Sci. **544**, 183 (2003).
[21] T. J. Oliveira and F. D. A. Aarao Reis, J. Appl. Phys. **101**, 063507 (2007).